J. Fluid Mech. (2007), *vol.* 578, *pp.* 371–380.
doi:10.1017/S002211200700523X Printed in the United Kingdom

Asymptotic solutions of convection in rapidly rotating non-slip spheres

KEKE ZHANG[1], XINHAO LIAO[2] AND F. H. BUSSE[3]

[1]Department of Mathematical Sciences, University of Exeter, EX4 4QE, UK
[2]Shanghai Astronomical Observatory, Chinese Academy of Sciences, Shanghai 200030, China
[3]Institute of Physics, University of Bayreuth, D-95440 Bayreuth, Germany

(Received 12 October 2006 and in revised form 1 February 2007)

Asymptotic solutions describing the onset of convection in rotating, self-gravitating Boussinesq fluid spheres with no-slip boundary conditions, valid for asymptotically small Ekman numbers and for all values of the Prandtl number, are derived. Central to the asymptotic analysis is the assumption that the leading-order convection can be represented, dependent on the size of the Prandtl number, by either a single quasi-geostrophic-inertial-wave mode or by a combination of several quasi-geostrophic-inertial-wave modes, and is controlled or influenced by the effect of the oscillatory Ekman boundary layer. Comparisons between the asymptotic solutions and the corresponding fully numerical simulations show a satisfactory quantitative agreement.

1. Introduction

The problem of thermal convection in rapidly rotating, self-gravitating, internally heated Boussinesq fluid spheres is characterized by three physical parameters: the Rayleigh number R, the Prandtl number Pr and the Ekman number E. Motivated by geophysical and planetary physical applications, which are usually characterized by extremely small Ekman numbers ($E \leqslant 10^{-9}$) and moderately small Prandtl numbers ($0 < Pr < O(1)$), the convection problem in rapidly rotating spherical systems has been extensively studied (see, for example, Chandrasekhar 1961; Roberts 1968; Busse 1970; Soward 1977; Zhang 1995; Tilgner & Busse 1997; Jones, Soward & Mussa 2000; Christensen 2002; Dormy *et al.* 2004; Chan, Li & Liao 2006). A review article by Busse (2002) gives further references on the earlier studies of the problem. The present paper represents an attempt to derive asymptotic solutions in rotating fluid spheres with the no-slip velocity boundary condition, valid for $0 \leqslant Pr/E < \infty$ at an asymptotically small E.

It is important to note that there are no general asymptotic scalings for $E \ll 1$ appropriate to all values of Pr/E in rotating spheres with no-slip boundary conditions. For an arbitrary small but non-zero E, the asymptotic scalings $R_c = O(E^{1/2})$, $m_c = O(1)$ are valid in the limit $Pr/E \to 0$ (Zhang 1995), where R_c denotes the critical Rayleigh number and m_c is the corresponding azimuthal wavenumber at the onset of convection. In the opposite limit $Pr/E \to \infty$ the asymptotic scalings at leading order in rotating no-slip spheres are given by $R_c = O(E^{-1/3}), m_c = O(E^{-1/3})$ (Dormy *et al.* 2004). The asymptotic scalings in terms of small E, which dramatically simplify the mathematical analysis of the problem (see, for example, Roberts 1968; Busse 1970; Jones *et al.* 2000; Dormy *et al.* 2004), do not exist in the general asymptotic solutions for $0 \leqslant Pr/E < \infty$, implying that the general problem must involve solutions of the full partial differential equations in spherical geometry.

Our asymptotic solutions in rotating no-slip spheres for $0 \leqslant Pr/E < \infty$ at $E \ll 1$, following the method developed for stress-free spheres (Zhang & Liao 2004), are based on the three hypotheses: (i) the convective flow is quasi-geostrophic; (ii) the leading-order velocity can be represented by either a single quasi-geostrophic-inertial-wave (QGIW) mode or by a combination of QGIW modes for which explicit analytical expressions are available (Zhang *et al.* 2001); and (iii) there exists a strong Ekman boundary layer on the bounding spherical surface that either controls (when Pr is small or moderate) or modifies (when Pr is moderately large) the interior convective flow.

The three hypotheses and the related asymptotic analysis are closely associated with the underlying physics and dynamics of convection in rapidly rotating no-slip spheres: a single inviscid QGIW mode or several inviscid QGIW modes which are modified by viscous effects, mainly via the Ekman boundary layers at the spherical bounding surface, and which are energetically driven by thermal buoyancy against viscous dissipation. The unanswered mathematical question regarding the completeness of the inertial wave modes, raised by Greenspan (1968), is irrelevant to the present asymptotic analysis. The result of our asymptotic analysis not only confirms the proposed structure of the convective flow for $0 \leqslant Pr/E < \infty$ at $E \ll 1$ but also offers a natural bridge between two previously disjoint problems in rotating fluids: thermal convection and inviscid inertial waves.

2. Mathematical formulation and numerical analysis

Consider a Boussinesq fluid sphere of radius r_o with constant thermal diffusivity κ, thermal expansion coefficient α and kinematic viscosity ν. The fluid sphere rotates uniformly with a constant angular velocity $\boldsymbol{\Omega}$ in the presence of its own gravitational field, $-\gamma \boldsymbol{r}$, where γ is a positive constant and $\boldsymbol{r}$ is the position vector. The whole sphere is heated by a uniform distribution of heat sources (see, for example, Chandrasekhar 1961; Roberts 1968; Busse 1970; Soward 1977; Jones *et al.* 2000), producing the unstable conducting temperature gradient $-\beta \boldsymbol{r}$, β being a positive constant. The problem of thermal convection is then governed by the three dimensionless equations

$$\frac{\partial \boldsymbol{u}}{\partial t} + \boldsymbol{u} \cdot \nabla \boldsymbol{u} + 2\boldsymbol{k} \times \boldsymbol{u} = -\nabla p + R\Theta \boldsymbol{r} + E\nabla^2 \boldsymbol{u}, \tag{2.1}$$

$$(Pr/E)\left(\frac{\partial \Theta}{\partial t} + \boldsymbol{u} \cdot \nabla \Theta\right) = \boldsymbol{u} \cdot \boldsymbol{r} + \nabla^2 \Theta, \tag{2.2}$$

$$\nabla \cdot \boldsymbol{u} = 0, \tag{2.3}$$

where $\boldsymbol{k}$ is a unit vector parallel to the axis of rotation, Θ represents the deviation of the temperature from its static distribution, p is the total pressure and $\boldsymbol{u}$ is the three-dimensional velocity field, $\boldsymbol{u} = (u_r, u_\theta, u_\phi)$ in spherical polar coordinates (r, θ, ϕ) with unit vectors $(\hat{\boldsymbol{r}}, \hat{\boldsymbol{\theta}}, \hat{\boldsymbol{\phi}})$. We have employed the radius of the sphere r_o as the length scale, $1/\Omega$ as the unit of time and $\beta r_o^4 \Omega/\kappa$ as the unit of temperature fluctuation Θ. The three non-dimensional parameters, the Rayleigh number R, the Prandtl number Pr and the Ekman number E, are defined as

$$R = \frac{\alpha\beta\gamma r_o^4}{\Omega\kappa}, \qquad Pr = \frac{\nu}{\kappa}, \qquad E = \frac{\nu}{\Omega r_o^2}.$$

The rigid, no-slip boundary with fixed temperature assumed in this paper gives rise to the conditions

$$u_r = u_\theta = u_\phi = \Theta = 0 \quad \text{at } r = 1. \tag{2.4}$$

The amplitude of convection is assumed to be sufficiently small to neglect the nonlinear terms. The corresponding linear equations describing the onset of convection, subject to the boundary conditions (2.4), will be solved numerically for a spherical shell with a small inner core as well as asymptotically ($E \ll 1$) for the full sphere.

The primary purpose of the fully numerical analysis, valid for any value of the Ekman number E, is to compare with the asymptotic solutions valid only for $E \ll 1$. In the numerical simulations, we expand the velocity $\boldsymbol{u}$ as a sum of poloidal (v) and toroidal vectors (w)

$$\boldsymbol{u} = [\nabla \times \nabla \times \boldsymbol{r} v(r, \theta, \phi) + \nabla \times \boldsymbol{r} w(r, \theta, \phi)]\, \mathrm{e}^{2\mathrm{i}\sigma t}, \tag{2.5}$$

where σ is the half-frequency. We then solve the three independent non-dimensional scalar equations,

$$\left[E\nabla^2 + 2(1-\eta)^2\left(\frac{\partial}{\partial\phi} - \mathrm{i}\sigma\mathscr{L}\right)\right]\nabla^2 v + 2(1-\eta)^2\mathscr{Q}w - (1-\eta)^6 R\mathscr{L}\Theta = 0, \tag{2.6}$$

$$\left[E\nabla^2 + 2(1-\eta)^2\left(\frac{\partial}{\partial\phi} - \mathrm{i}\sigma\mathscr{L}\right)\right]w - 2(1-\eta)^2\mathscr{Q}v = 0, \tag{2.7}$$

$$[E\nabla^2 - 2\mathrm{i}(1-\eta)^2\sigma Pr]\Theta + E\mathscr{L}v = 0, \tag{2.8}$$

where η is the ratio of the inner sphere radius (r_i) to the outer sphere radius (r_o), $\eta = r_i/r_o$, and the differential operators $\mathscr{L}$ and $\mathscr{Q}$ are defined as

$$\mathscr{L} = -r^2\nabla^2 + \frac{\partial}{\partial r}r^2\frac{\partial}{\partial r}, \qquad \mathscr{Q} = \boldsymbol{k}\cdot\nabla - \tfrac{1}{2}(\mathscr{L}\boldsymbol{k}\cdot\nabla + \boldsymbol{k}\cdot\nabla\mathscr{L}).$$

In the numerical simulations the inner sphere is set to be sufficiently small, giving $\eta = 0.01$ to facilitate its comparison with the full sphere. The boundary conditions (2.4) concerning v, w and Θ in a spherical shell are

$$v = \frac{\partial v}{\partial r} = w = \Theta = 0 \quad \text{at} \quad r_i = \frac{\eta}{(1-\eta)}, \quad r_o = \frac{1}{(1-\eta)}. \tag{2.9}$$

We then solve the governing equations by expanding the velocity potentials and temperature in terms of spherical harmonics ($P_l^m(\cos\theta)\,\mathrm{e}^{\mathrm{i}m\phi}$) and of radial functions that satisfy the no-slip boundary condition,

$$w = \sum_{l,n} w_{ln}\left[1 - \left(2r - \frac{1+\eta}{1-\eta}\right)^2\right]T_n\left(2r - \frac{1+\eta}{1-\eta}\right)P_l^m(\cos\theta)\,\mathrm{e}^{\mathrm{i}m\phi}, \tag{2.10}$$

$$v = \sum_{l,n} v_{ln}\left[1 - \left(2r - \frac{1+\eta}{1-\eta}\right)^2\right]^2 T_n\left(2r - \frac{1+\eta}{1-\eta}\right)P_l^m(\cos\theta)\,\mathrm{e}^{\mathrm{i}m\phi}, \tag{2.11}$$

$$\Theta = \sum_{l,n} \Theta_{ln}\left[1 - \left(2r - \frac{1+\eta}{1-\eta}\right)^2\right]T_n\left(2r - \frac{1+\eta}{1-\eta}\right)P_l^m(\cos\theta)\,\mathrm{e}^{\mathrm{i}m\phi}, \tag{2.12}$$

where $T_n(x)$ denotes the standard Chebyshev function. The spherical harmonics are normalized,

$$\frac{1}{4\pi}\int_0^{2\pi}\int_0^{\pi}\left|P_l^m(\cos\theta)\,\mathrm{e}^{\mathrm{i}m\phi}\right|^2\sin\theta\,\mathrm{d}\theta\,\mathrm{d}\phi = 1,$$

and $w_{ln}, v_{ln}, \Theta_{ln}$ are complex coefficients to be determined numerically. The fully numerical solutions obtained for various Prandtl numbers at $E \ll 1$ will be discussed later together with the corresponding asymptotic solutions.

3. Asymptotic solutions for $E \ll 1$

In rapidly rotating spheres with the no-slip conditions, an asymptotic solution $\boldsymbol{u}$ of convection can be separated at leading order into the interior flow $\boldsymbol{u}_0$ and the Ekman-boundary-layer flow $\boldsymbol{u}_b$, i.e. $\boldsymbol{u} = \boldsymbol{u}_0 + \boldsymbol{u}_b$ (see, for example, Greenspan 1968).

We first look at the interior convective flow $\boldsymbol{u}_0$. The hypotheses for the asymptotic solution at $E \ll 1$ lead to an expansion for the velocity $\boldsymbol{u}_0$ and the pressure p_0 in the form

$$\boldsymbol{u}_0 = \sum_N C_N(\boldsymbol{U}_N + \tilde{\boldsymbol{u}}_N)\,\mathrm{e}^{2\mathrm{i}\sigma t}, \quad p_0 = \sum_N C_N(P_N + \tilde{p}_N)\,\mathrm{e}^{2\mathrm{i}\sigma t}, \tag{3.1}$$

where C_N are complex coefficients, $\tilde{\boldsymbol{u}}_N$ and $\tilde{p}_N$ denote the interior perturbations induced by the flux from the oscillatory Ekman boundary layer, σ is the half-frequency of convection and $\boldsymbol{U}_N$, P_N represent a QGIW mode satisfying

$$2(\mathrm{i}\sigma_N \boldsymbol{U}_N + \boldsymbol{k} \times \boldsymbol{U}_N) + \nabla P_N = 0, \qquad \nabla \cdot \boldsymbol{U}_N = 0, \tag{3.2}$$

which are subject to $\hat{\boldsymbol{r}} \cdot \boldsymbol{U}_N = 0$ at $r = 1$. Also, $\boldsymbol{U}_N$ has the equatorial symmetry

$$(U_{N\phi}, U_{Nr}, U_{N\theta})(\theta) = (U_{N\phi}, U_{Nr}, -U_{N\theta})(\pi - \theta), \tag{3.3}$$

and is nearly independent of $r\cos\theta$ (i.e. quasi-geostrophic with $|\sigma_N| \ll 1$, except for the case $Pr/E \ll 1$) and described by a polynomial of degree $2N$. Explicit expressions for all $\boldsymbol{U}_N$ and some typical values of σ_N, as well as the equation for the determination of all σ_N, can be found in Zhang *et al.* (2001). At the edge of the spherical Ekman boundary layer, the radial component of the interior flow $\boldsymbol{u}_0$ is characterized by

$$\hat{\boldsymbol{r}} \cdot \boldsymbol{u}_0 = O\left(E^{1/2}\right), \tag{3.4}$$

which is needed for asymptotic matchings for the general asymptotic solution.

We then look at the oscillatory Ekman boundary flow $\boldsymbol{u}_b$ on the spherical bounding surface. For a sufficiently small E, the Ekman boundary flow $\boldsymbol{u}_b$ is governed by

$$2\mathrm{i}\sigma \boldsymbol{u}_b + 2\boldsymbol{k} \times \boldsymbol{u}_b - \hat{\boldsymbol{r}} \frac{\partial p_b}{\partial \xi} = \frac{\partial^2 \boldsymbol{u}_b}{\partial \xi^2}, \tag{3.5}$$

where ξ represents the stretched boundary-layer variable, $\xi = E^{-1/2}(1-r)$, for $E \ll 1$: $\xi = 0$ is at the bounding no-slip surface and $\xi \to \infty$ defines the edge of the Ekman boundary layer. The above equation can be reduced to a fourth-order differential equation for $\boldsymbol{u}_b$ (see, for example, Kudlick 1966),

$$\left(\frac{\partial^2}{\partial \xi^2} - 2\mathrm{i}\sigma\right)^2 \boldsymbol{u}_b + 4(\boldsymbol{k} \cdot \hat{\boldsymbol{r}})^2 \boldsymbol{u}_b = 0, \tag{3.6}$$

which can be solved subject to four boundary conditions. The first two boundary conditions are on the no-slip surface at $\xi = 0$,

$$[\boldsymbol{r} \times \boldsymbol{u}_b]_{\xi=0} + \sum_N C_N [\boldsymbol{r} \times \boldsymbol{U}_N]_{r=1} = 0, \tag{3.7}$$

$$\left[\frac{\partial^2 \boldsymbol{u}_b}{\partial \xi^2}\right]_{\xi=0} + \sum_N 2C_N [\mathrm{i}\sigma \boldsymbol{U}_N + (\boldsymbol{k} \cdot \hat{\boldsymbol{r}})\hat{\boldsymbol{r}} \times \boldsymbol{U}_N]_{r=1} = 0. \tag{3.8}$$

The other two are at the edge of the Ekman boundary layer flow, evaluated at $\xi = \infty$,

$$[\hat{\boldsymbol{r}} \times \hat{\boldsymbol{u}}_b]_{\xi=\infty} = 0, \qquad \left[\frac{\partial^2 \boldsymbol{u}_b}{\partial \xi^2}\right]_{\xi=\infty} = 0. \tag{3.9}$$

A straightforward but cumbersome analysis shows that the leading-order boundary-layer solution on the bounding no-slip spherical surface is given by

$$\boldsymbol{u}_b = -\sum_N C_N \left[\frac{B_N^+}{2}(\mathrm{i}\hat{\boldsymbol{\theta}} + \hat{\boldsymbol{\phi}}) \exp(Z_N^+ \xi) + \frac{B_N^-}{2}(\mathrm{i}\hat{\boldsymbol{\theta}} - \hat{\boldsymbol{\phi}}) \exp(Z_N^- \xi) \right] \exp(\mathrm{i}m\phi + \mathrm{i}2\sigma t), \quad (3.10)$$

where

$$Z_N^{\pm} = -\left[1 + \frac{(\sigma_N \pm \cos\theta)}{|\sigma_N \pm \cos\theta|}\mathrm{i}\right] \sqrt{|\sigma_N \pm \cos\theta|},$$

$$B_N^{\pm} = \sum_{i=0}^{N} \sum_{j=0}^{N-i} \frac{C_{ijmN}}{Q_N} \left[\sigma_N^{2i-1}(1-\sigma_N^2)^{j-1} \sin^{m+2j-1}\theta \cos^{2i-1}\theta\right]$$
$$\times \left[-\sigma_N(m + m\sigma_N + 2j\sigma_N)\cos^2\theta - 2i\left(1-\sigma_N^2\right)\sin^2\theta \pm \sigma_N(m + m\sigma_N + 2j)\cos\theta\right],$$

with C_{ijmN} being defined as

$$C_{ijmN} = \frac{(-1)^{i+j}[2(N+i+j+m)-1]!!}{2^{j+1}(2i-1)!!(N-i-j)!i!j!(m+j)!},$$

where $n! = n(n-1)\ldots(2)(1)$, $(2n-1)!! = (2n-1)(2n-3)\ldots(3)(1)$, and Q_N is the normalization factor

$$Q_N^2 = \sum_{i=0}^{N} \sum_{j=0}^{N-i} \sum_{k=0}^{N} \sum_{l=0}^{N-k} 2^{j+l+m-1} C_{ijmN} C_{klmN} \sigma_N^{2(i+k-1)} \left(1-\sigma_N^2\right)^{j+l-1}$$
$$\times \frac{(m+j+l-1)!(2i+2k-3)!!}{[2(m+j+l+i+k)+1)!!} \left[8ik(m+j+l)\left(1-\sigma_N^2\right) + \sigma_N^2(2j\sigma_N + m\sigma_N + m)\right.$$
$$\left. \times (2l\sigma_N + m\sigma_N + m) + (2j + m\sigma_N + m)(2l + m\sigma_N + m)(2i + 2k - 1)\right], \quad (3.11)$$

which is chosen such that $\langle |\boldsymbol{U}_N|^2 \rangle = 1$, $\langle\ \rangle$ denoting the volume integral over the sphere. Obviously, the solution for the spherical Ekman boundary layer (3.10) is not determined at this stage because of the undetermined coefficients C_N in the expression. It should also be noted that the boundary-layer solution breaks down at the critical latitudes $\theta_c = \cos^{-1}\sigma_N$, i.e. the Ekman boundary layer would be locally thickened at the critical latitudes. However, the local thickening of the Ekman layer does not appear to affect significantly the leading-order global solution in a full sphere (see, for example, Hollerbach & Kerswell 1995; Zhang 1995) and we shall neglect the local-thickening effects on the asymptotic convection solutions.

An asymptotic convection solution, described by the Rayleigh number R, the half-frequency σ and the coefficients C_N, is determined by matching the interior solution $\boldsymbol{u}_0$ to the boundary-layer solution $\boldsymbol{u}_b$ at the edge of the Ekman boundary layer. Substituting (3.1) into the momentum equation, multiplying the result by $\boldsymbol{U}_M^*$, the complex conjugate of $\boldsymbol{U}_M$, making use of the boundary-layer solution (3.10) and integrating the resulting equation over the sphere, we obtain a system of algebraic equations for C_N, R and σ:

$$C_M \mathrm{i}(\sigma - \sigma_M) + \sum_N C_N(E\mathscr{F}_{MN} - R\mathscr{G}_{MN})$$
$$= -\pi E^{1/2} \left\{ \sum_N C_N \int_0^{\pi} \frac{B_N^+}{\sqrt{|\sigma_N + \cos\theta|}} \left[\frac{(\sigma_N + \cos\theta)}{|\sigma_N + \cos\theta|} + \mathrm{i}\right] \left(\sin\theta \frac{\partial P_M}{\partial\theta} - m P_M\right) \mathrm{d}\theta \right\} \quad (3.12)$$

for $M = 1, 2, 3, \ldots$. Here $\mathscr{F}_{MN}$ is related to the internal viscous dissipation and given by

$$\begin{aligned}\mathscr{F}_{MN} &= \langle \nabla \times \boldsymbol{U}_M^* \cdot \nabla \times \boldsymbol{U}_N \rangle \\ &= \sum_{i=0}^{N} \sum_{j=0}^{N-i} \sum_{k=0}^{M} \sum_{l=0}^{M-k} 2^{j+l+m-1} \frac{C_{ijmN}}{Q_N} \frac{C_{klmM}}{Q_M} \sigma_N^{2i-1} \sigma_M^{2k-1} \left(1-\sigma_N^2\right)^{j-1} \left(1-\sigma_M^2\right)^{l-1} \\ &\quad \times \frac{(m+j+l-1)!(2i+2k-3)!!}{[2(m+j+l+i+k)-1]!!} \{8ik(2i-1)(2k-1)(m+j+l)\left(1-\sigma_N^2\right)\left(1-\sigma_M^2\right) \\ &\quad + 4ik\sigma_N\sigma_M[2j\sigma_N + m\sigma_N + m)(2l\sigma_N + m\sigma_N + m) \\ &\quad + (2j + m\sigma_N + m)(2l + m\sigma_N + m)](2i + 2k - 3)\},\end{aligned}$$

P_M describes the pressure distribution at the edge of the Ekman boundary layer,

$$P_M = \sum_{i=0}^{M} \sum_{j=0}^{M-i} \frac{2C_{ijmM}}{Q_M} \sigma_M^{2i} \left(1-\sigma_M^2\right)^j \sin^{m+2j}\theta \cos^{2i}\theta,$$

and $\mathscr{G}_{MN}$ represents the thermal effect of convection

$$\begin{aligned}\mathscr{G}_{MN} &= \langle \boldsymbol{U}_M^* \cdot \boldsymbol{r}\Theta \rangle \\ &= \sum_{l,k} \frac{\left(E\xi_{lk}^2 - \mathrm{i}\sigma Pr\right) \langle \boldsymbol{U}_M^* \cdot \boldsymbol{r} P_l^m j_l(\xi_{lk} r) \rangle \langle \boldsymbol{U}_N \cdot \boldsymbol{r} P_l^m j_l(\xi_{lk} r) \rangle}{2\pi\left(E^2\xi_{lk}^4 + \sigma^2 Pr^2\right) j_{l+1}^2(\xi_{lk})},\end{aligned}$$

where $j_l(\xi_{lk} r)$ are the spherical Bessel functions with ξ_{lk} being chosen such that $j_l(\xi_{lk}) = 0$ and $0 < \xi_{l1} < \xi_{l2} < \xi_{l3} \ldots$. In deriving (3.12), we have made an assumption that in

$$\langle \boldsymbol{U}_M^* \cdot \nabla^2 \boldsymbol{u}_0 \rangle = -\sum_N C_N \langle \nabla \times \boldsymbol{U}_M^* \cdot \nabla \times \boldsymbol{U}_N \rangle + \int_S \boldsymbol{U}_M^* \cdot [(\nabla \times \boldsymbol{u}_0) \times \hat{\boldsymbol{r}}] \, \mathrm{d}S \qquad (3.13)$$

the surface integral on the right-hand side, in comparison to the preceding volume integral, can be neglected. For prescribed values of E, m, Pr, (3.12) can be readily solved to determine the values of R, σ and the complex coefficients C_N, $N = 1, 2, 3 \ldots$, describing the onset of convection in rotating no-slip spheres. The smallest Rayleigh number, denoted by a subscript c, represents the critical or most unstable mode of convection in a rapidly rotating no-slip sphere.

In the limit $Pr/E \to 0$, (3.12) becomes particularly simple because different QGIW modes are completely decoupled. In this case, the summation in (3.12) reduces to a single equation with one QGIW mode U_K and the half-frequency σ_K, leading to

$$R = \frac{E^{1/2}}{\mathscr{G}_{KK}} \left[\pi \int_0^\pi B_K^+ \frac{(\sigma_K + \cos\theta)}{|\sigma_K + \cos\theta|^{3/2}} \left(\sin\theta \frac{\partial P_K}{\partial \theta} - m P_K \right) \mathrm{d}\theta + E^{1/2} \mathscr{F}_{KK} \right], \qquad (3.14)$$

$$\sigma = \sigma_K - E^{1/2}\pi \left[\int_0^\pi \frac{B_K^+}{\sqrt{|\sigma_K + \cos\theta|}} \left(\sin\theta \frac{\partial P_K}{\partial \theta} - m P_K \right) \mathrm{d}\theta \right]. \qquad (3.15)$$

Minimization of R over different QGIW modes, with various values of K and m, yields the critical parameters describing the most unstable mode in rapidly rotating no-slip spheres when $Pr/E \ll 1$. In this case, it is found that the onset of convection obeys the asymptotic relations,

$$m_c = 1, \quad R_c = E^{1/2}\left(8.868 \times 10^2 + 1.033 \times 10^4 E^{1/2}\right), \quad \sigma_c = 0.7550 + 0.2177 E^{1/2}, \qquad (3.16)$$

while other QGIW modes give rise to larger Rayleigh numbers and thus are not preferred. For instance, the QGIW mode with $m=2$, $K=1$ and $\sigma_1=0.6160$ results in

$$m=2, \quad R=E^{1/2}\left(1.298\times10^3+1.915\times10^4E^{1/2}\right), \quad \sigma_c=0.6160+0.2020E^{1/2}. \tag{3.17}$$

The asymptotic relations can be compared with the corresponding fully numerical simulations at $Pr=0$ for different values of E. At $E=10^{-4}$, the asymptotic solution (3.16) gives $R_c=9.90$, $\sigma_c=0.757$ while the fully numerical analysis yields $R_c=9.42$, $\sigma_c=0.756$. At the smaller Ekman number $E=10^{-5}$, the asymptotic solution (3.16) gives $R_c=2.91$, $\sigma_c=0.756$ while the fuller numerics yields $R_c=2.90$, $\sigma_c=0.755$. A satisfactory agreement between the asymptotic relations (3.16) and the direct numerical solution has thus been achieved. Moreover, the explicit analytical convection flow in a rotating no-slip sphere for $Pr/E\ll1$ can be written in the complex form

$$u_r = \mathrm{i}\sin\theta[r^2-1]\mathrm{e}^{\mathrm{i}(\phi+2\sigma_1 t)}, \tag{3.18}$$

$$\begin{aligned} u_\phi = \Big\{ & [1-2r^2-gr^2(\cos^2\theta-\sin^2\theta)]-[(1-\cos\theta) \\ & \times(-1-g(\cos^2\theta-\sin^2\theta)/2)+2g\sin^2\theta\cos\theta] \\ & \times\mathrm{e}^{(1-r)Z_1^+E^{-1/2}}-[(1+\cos\theta)(-1-g(\cos^2\theta-\sin^2\theta))/2 \\ & -2g\sin^2\theta\cos\theta]\mathrm{e}^{(1-r)Z_1^-E^{-1/2}}\Big\}\mathrm{e}^{\mathrm{i}(\phi+2\sigma_1 t)}, \end{aligned} \tag{3.19}$$

$$\begin{aligned} u_\theta = \Big\{ & [(2-g)r^2-1]\cos\theta-[(1-\cos\theta) \\ & \times(-1-g(\cos^2\theta-\sin^2\theta))/2+2g\sin^2\theta\cos\theta] \\ & \times\mathrm{e}^{(1-r)Z_1^+E^{-1/2}}+[(1+\cos\theta)(-1-g(\cos^2\theta-\sin^2\theta))/2 \\ & -g\sin^2\theta\cos\theta]\mathrm{e}^{(1-r)Z_1^-E^{-1/2}}\Big\}\mathrm{i}\mathrm{e}^{\mathrm{i}(\phi+2\sigma_1 t)}, \end{aligned} \tag{3.20}$$

where the abbreviation $g\equiv\frac{4}{9}\sqrt{10}-\frac{5}{9}$ has been used and

$$\sigma_1=\frac{1}{3}\left(1+2\sqrt{\frac{2}{5}}\right)=0.7550, \quad Z_1^\pm=-\left[1+\frac{(\sigma_1\pm\cos\theta)}{|\sigma_1\pm\cos\theta|}\mathrm{i}\right]|\sigma_1\pm\cos\theta|^{1/2}.$$

When Pr increases from the limit $Pr/E\to0$, equation (3.12) suggests several important effects. When $Pr/E\ll1$, the term relating to the Ekman boundary layer, proportional to $E^{1/2}$ on the right-hand side of (3.12), plays an essential role in controlling the behaviour of convection. In the limit $Pr/E\to\infty$, the term relating to the internal viscous dissipation, proportional to E on the left-hand side of (3.12), plays a leading role (see, for example, Jones *et al.* 2000; Dormy *et al.* 2004). However, generally speaking, all the terms in (3.12) are important when Pr is not within the asymptotic limits. It is also expected that more than one QGIW mode would be excited and sustained by thermal convection because the viscous effect, measured by a non-zero Pr in (3.12), couples a dominant QGIW mode with the neighbouring QGIW modes having frequencies close to that of the dominant mode.

For given values of E and Pr, we can calculate various convection modes by solving (3.12) with a Newton–Raphson iterative procedure to determine the critical mode corresponding to the smallest Rayleigh number R_c. Table 1 shows two sets of the critical Rayleigh number R_c, the corresponding wavenumber m_c and half-frequency σ_c

Pr	$(R_c, m_c, \sigma_c)_{FNUM}$	$(R_c, m_c, \sigma_c)_{QGIW}$
0.001	(23.74, 2, −0.1064)	(22.14, 2, −0.1095)
0.01	(36.50, 2, −0.0927)	(35.42, 2, −0.0957)
0.05	(74.45, 4, −0.0466)	(74.65, 4, −0.0458)
0.1	(95.34, 5, −0.0394)	(94.17, 5, −0.0390)
0.25	(143.3, 6, −0.0269)	(140.8, 6, −0.0272)
0.7	(226.7, 7, −0.0145)	(225.7, 7, −0.0155)
1.0	(258.6, 7, −0.0108)	(257.9, 7, −0.0114)

TABLE 1. The critical Rayleigh numbers R_c, the preferred wavenumbers m_c and half-frequencies σ_c at the onset of convection at $E = 10^{-4}$ for various Prandtl numbers. The fully numerical solutions in a rotating spherical shell with a small inner sphere at $r_i/r_o = 0.01$ are indicated by the subscript $FNUM$ while the asymptotic solutions in a sphere by the subscript $QGIW$.

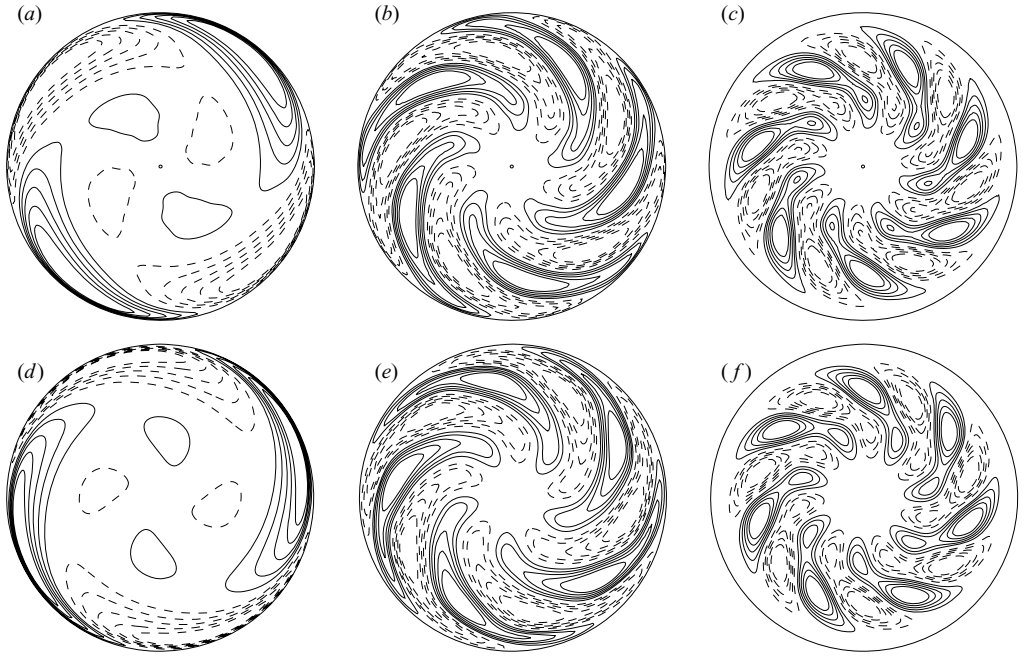

FIGURE 1. Contours of u_ϕ in the equatorial plane for three different Prandtl numbers at $E = 10^{-4}$: (*a, d*) for $Pr = 10^{-2}$, (*b, e*) for $Pr = 10^{-1}$, and (*c, f*) for $Pr = 1$. The upper panels show the fully numerical solutions in a rotating spherical shell with a small inner core while the lower panels show the asymptotic solutions in a rotating sphere.

obtained at $E = 10^{-4}$ for various values of Pr. The second set (with subscript $QGIW$) is obtained from the asymptotic solutions in the full sphere and the first set (with subscript $FNUM$) is calculated from fully numerical simulations in a spherical shell with a small inner core, showing a satisfactory agreement between the asymptotic and fully numerical solutions for all values of Pr/E. Figure 1 illustrates the typical structure of convection for three Prandtl numbers, $Pr = 0.01, 0.1, 1.0$, obtained from both the asymptotic solutions and numerical simulations, revealing nearly the same features.

The coefficients $|C_N|$ and their corresponding half-frequencies σ_N for the dominant QGIW modes are presented in table 2. Note that the degree of the polynomial

$(N, \lvert C_N\rvert, \sigma_N)$ for $Pr=10^{-2}$	$(N, \lvert C_N\rvert, \sigma_N)$ for $Pr=10^{-1}$	$(N, \lvert C_N\rvert, \sigma_N)$ for $Pr=1$
(1, 1.000, −0.1160)	(3, 1.000, −0.0435)	(3, 1.000, −0.0473)
(2, 0.443, −0.0509)	(2, 0.972, −0.0689)	(4, 0.880, −0.0339)
(3, 0.130, −0.0288)	(4, 0.628, −0.0303)	(2, 0.665, −0.0719)
	(1, 0.286, −0.1316)	(5, 0.512, −0.0257)
	(5, 0.242, −0.0224)	(3, 0.229, +0.2229)
	(2, 0.121, +0.3146)	(4, 0.193, +0.1921)
	(3, 0.117, +0.2569)	(2, 0.172, +0.2690)
		(6, 0.159, −0.0202)
		(5, 0.125, +0.1694)

TABLE 2. Dominant coefficients $|C_N|$ and the corresponding half-frequencies σ_N derived from (3.12) for three convection solutions with three Prandtl numbers, $Pr=0.01, 0.1, 1$, at $E=10^{-4}$. Smaller coefficients with $|C_N| < 0.1$ are not shown.

for a QGIW mode $\boldsymbol{U}_N$ is $2N$. At $Pr=0.01$, the convection is dominated by a single QGIW mode (a polynomial of degree 2) with $N=1, \sigma_1=-0.116$ and modified mainly by two QGIW modes with $N=2, \sigma_2=-0.051$ and $N=3, \sigma_3=-0.0288$. When the Prandtl number increases to $Pr=0.1$, the asymptotic solution becomes dominated by the two QGIW modes with $N=3, \sigma_3=-0.0435$ (with a polynomial of degree 6) and $N=2, \sigma_2=0.0688$ (with a polynomial of degree 4). It is important to note that the viscous coupling of different QGIW modes causes the spiralling structure of convection illustrated in figure 1. At $Pr=1.0$, the chief dominant QGIW modes are shifted to $N=3, 4, 2$ with the critical azimuthal wavenumber $m_c=7$. By inserting the values of the coefficients C_N given in table 2 into (3.1) for the interior flow $\boldsymbol{u}_0$ and into (3.10) for the boundary-layer flow $\boldsymbol{u}_b$, we obtain an approximate explicit asymptotic solution of convection $(\boldsymbol{u}_0+\boldsymbol{u}_b)$ in a rotating sphere satisfying the no-slip conditions (2.4).

4. Summary and remarks

We have presented asymptotic solutions for $E \ll 1$ in rotating spheres with no-slip boundary conditions. The asymptotic analysis hinges primarily on the assumption that the leading-order velocity of convection can be represented, dependent on the size of the the Prandtl number, by either a single QGIW mode or by a number of QGIW modes, and is either controlled or modified by the Ekman-boundary-layer flux. We found a satisfactory agreement between the asymptotic and the direct numerical solutions for $E \ll 1$ and a wide range of Prandtl numbers. More fundamentally, our asymptotic solutions point to the underlying structure and dynamics of convection in rapidly rotating no-slip fluid spheres.

A potentially important advantage of the current asymptotic approach is that it may be readily extended to include the effect of compressibility, because the problem of inertial waves in rotating compressible fluids can be reformulated under the anelastic approximation (Busse, Zhang & Liao 2005). We can re-write the equations for the velocity $\hat{\boldsymbol{u}}_0$ of compressible convection under the anelastic approximation in the form

$$\frac{\partial\,(\rho_0\hat{\boldsymbol{u}}_0)}{\partial t} + 2\boldsymbol{k}\times(\rho_0\hat{\boldsymbol{u}}_0) + \nabla\hat{p}_0 = 0, \qquad \nabla\cdot(\rho_0\hat{\boldsymbol{u}}_0) = 0, \tag{4.1}$$

where ρ_0 represents the density distribution depending on r only. The relationship between the internal convection solutions in the Boussinesq fluid $(\boldsymbol{u}_0)$ and in the

compressible fluid ($\hat{\boldsymbol{u}}_0$) is then simply given by

$$\hat{\boldsymbol{u}}_0(r,\theta,\phi,t) = \frac{1}{\rho_0(r)}\boldsymbol{u}_0(r,\theta,\phi,t) = \frac{1}{\rho_0(r)}\left[\sum_N C_N \boldsymbol{U}_N\right] \mathrm{e}^{2\mathrm{i}\sigma t}. \tag{4.2}$$

For a given $\rho_0(r)$, the asymptotic analysis can be carried out in a similar way to that in this paper. Of course the analysis would be much more complicated and lengthy and the values of the critical Rayleigh number and other parameters will be modified by the compressible effects.

K. Z. is supported by PPARC, NERC and Leverhulme grants and X. L. is supported by NSFC grant/10633030. Computation is supported by Shanghai Super Computer Centre.

REFERENCES

Busse, F. H. 1970 Thermal instabilities in rapidly rotating systems. *J. Fluid Mech.* **44**, 441–460.

Busse, F. H. 2002 Convective flows in rapidly rotating spheres and their dynamo action. *Phys. Fluids* **14**, 1301–1314.

Busse, F. H., Zhang, K. & Liao, X. 2005 On slow inertial waves in the solar convection zone. *Astrophys. J.* **631**, L171–L174.

Chan, K. H. Li, L. & Liao, X. 2006. Modelling the core convection using finite element and finite difference methods. *Phys. Earth Planet. Inter.* **157**, 124–138.

Chandrasekhar, S. 1961 *Hydrodynamic and Hydromagnetic Stability*. Clarendon.

Christensen, U. R. 2002 Zonal flow driven by strongly supercritical convection in rotating spherical shells *J. Fluid Mech.* **470**, 115–133.

Dormy, A. M., Soward, A. M., Jones, C. A., Jault, D. & Cardin, P. 2004 The onset of thermal convection in rotating spherical shells. *J. Fluid Mech.* **501**, 43–70.

Greenspan, H. P. 1968 *The Theory of Rotating Fluids*. Cambridge University Press.

Hollerbach, R. & Kerswell, R. R. 1995 Oscillatory internal shear layers in rotating and precessing flows. *J. Fluid Mech.* **298**, 327–339.

Jones, C. A., Soward, A. M. & Mussa, A. I. 2000 The onset of thermal convection in a rapidly rotating sphere. *J. Fluid Mech.* **405**, 157–179.

Kudlick, M. D. 1966 On transient motions in a contained, rotating fluid. PhD Thesis, Department of Mathematics, MIT.

Roberts, P. H. 1968 On the thermal instability of a self-gravitating fluid sphere containing heat sources. *Phil. Trans. R. Soc. Lond.* A **263**, 93–117.

Soward, A. M. 1977 On the finite amplitude thermal instability of a rapidly rotating fluid sphere. *Geophys. Astrophys. Fluid Dyn.* **9**, 19–74.

Tilgner, A. & Busse, F. H. 1997 Finite amplitude convection in rotating spherical fluid shells. *J. Fluid Mech.* **332**, 359–376

Zhang, K. 1995 On coupling between the Poincaré equation and the heat equation: non-slip boundary condition. *J. Fluid Mech.* **284**, 239–256.

Zhang, K., Earnshaw, P., Liao, X. & Busse, F. H. 2001 On inertial waves in a rotating fluid sphere. *J. Fluid Mech.* **437**, 103–119.

Zhang, K. & Liao, X. 2004 A new asymptotic method for the analysis of convection in a rotating sphere. *J. Fluid Mech.* **518**, 319–346.